Molecular Therapy
Methods & Clinical Development
Original Article

Antigen modifications improve nucleoside-modified mRNA-based influenza virus vaccines in mice

Alec W. Freyn,[1,2,6] Matthew Pine,[3] Victoria C. Rosado,[1] Marcel Benz,[1] Hiromi Muramatsu,[3] Mitchell Beattie,[4] Ying K. Tam,[4] Florian Krammer,[1] Peter Palese,[1,5] Raffael Nachbagauer,[1,6] Meagan McMahon,[1] and Norbert Pardi[3]

[1]Department of Microbiology, Icahn School of Medicine at Mount Sinai, New York, NY 10029, USA; [2]Graduate School of Biomedical Sciences, Icahn School of Medicine at Mount Sinai, New York, NY 10029, USA; [3]Department of Medicine, University of Pennsylvania, Philadelphia, PA 19104, USA; [4]Acuitas Therapeutics, Vancouver, BC V6T 1Z3, Canada; [5]Department of Medicine, Icahn School of Medicine at Mount Sinai, New York, NY 10029, USA

Nucleoside-modified, lipid nanoparticle-encapsulated mRNAs have recently emerged as suitable vaccines for influenza viruses and other pathogens in part because the platform allows delivery of multiple antigens in a single immunization. mRNA vaccines allow for easy antigen modification, enabling rapid iterative design. We studied protein modifications such as mutating functional sites, changing secretion potential, and altering protein conformation, which could improve the safety and/or potency of mRNA-based influenza virus vaccines. Mice were vaccinated intradermally with wild-type or mutant constructs of influenza virus hemagglutinin (HA), neuraminidase (NA), matrix protein 2 (M2), nucleoprotein (NP), or matrix protein 1 (M1). Membrane-bound HA constructs elicited more potent and protective antibody responses than secreted forms. Altering the catalytic site of NA to reduce enzymatic activity decreased reactogenicity while protective immunity was maintained. Disruption of M2 ion channel activity improved immunogenicity and protective efficacy. A comparison of internal proteins NP and M1 revealed the superiority of NP in conferring protection from influenza virus challenge. These findings support the use of the nucleoside-modified mRNA platform for guided antigen design for influenza virus with extension to other pathogens.

INTRODUCTION

Influenza viruses cause over half a million deaths annually, as well as millions of hospitalizations and subclinical infections.[1] Seasonal influenza virus vaccines confer suboptimal effectiveness due to poor immunogenicity or potential strain mismatches.[2] To overcome these obstacles to ideal care, broadly protective influenza virus vaccines are currently being developed, which offer the promise of superior and long-lasting immune responses.[3]

The influenza virus hemagglutinin (HA) conserved stalk domain has been a target of several vaccine strategies and human clinical trials,[4–7] as this region has been found to elicit antibodies with the ability to cross-react with multiple influenza A and B viruses and act to confer protection through direct neutralization and Fc-mediated effector functions.[8] Rationally designed vaccine candidates attempt to elicit this class of antibodies through sequential vaccination with chimeric HA proteins,[4] headless HA stalk-only constructs,[5,7] or hyperglycosylated HA head domain proteins.[9,10]

The viral neuraminidase (NA) has gained momentum as a potential vaccine antigen due to its ability to elicit antibodies that potently neutralize within a subtype.[11] Recently, broadly cross-reactive antibodies that target the NA active site have been discovered that can bind and inhibit influenza A and B viruses.[12] Strategies to supplement current influenza virus vaccines with NA components have been discussed to improve overall vaccine effectiveness.[13]

There have been several studies that have examined the potential of the extracellular domain of the matrix protein 2 (M2e) ion channel to serve as a universal influenza virus vaccine antigen.[14–16] The M2e region is highly conserved across influenza A viruses and is known to elicit non-neutralizing antibodies, which confer protection through antibody-dependent cell-mediated cytotoxicity (ADCC) activity.[15] The full-length M2 protein is also known to contain several T cell epitopes, which may act to enhance antibody responses or stimulate cellular immune responses.[14]

Strategies to stimulate broadly reactive cellular responses have also been investigated, often through the use of vectored expression of internal influenza virus proteins. Viral nucleoprotein (NP) and matrix protein 1 (M1) are favored antigens to stimulate cellular immunity due to the presence of highly conserved T cell epitopes.[17] Broadly cross-reactive cellular responses have been

Received 4 November 2020; accepted 4 June 2021;
https://doi.org/10.1016/j.omtm.2021.06.003.

[6]Present address: Moderna, 200 Technology Square, Cambridge, MA 02139, USA

Correspondence: Norbert Pardi, Department of Medicine, University of Pennsylvania, Philadelphia, PA 19104, USA.
E-mail: pnorbert@pennmedicine.upenn.edu

shown to lead to clearance of infected cells, which leads to a reduction in symptoms and viral transmission.[18] Vaccines that utilize these antigens as targets are currently being tested in clinical trials.[19]

Besides strain-specificity and limited potency, one of the major limitations of conventional influenza virus vaccine platforms is the difficulty with production in eggs or cell lines and the lack of flexibility to rapidly incorporate specific highly desired modifications.[20] Next-generation vaccine technologies have pushed the field of influenza vaccine development forward by allowing delivery of conserved antigens and preferentially skewing the immune system to provoke desired responses. Multiple preclinical studies provided proof-of-concept for the feasibility of mRNA-based vaccination against influenza virus.[21] Several studies utilized self-amplifying mRNA vaccines encoding HA, NP, or M1 antigens and demonstrated protection from lethal viral infection in mice and ferrets.[22,23] RNActive mRNA vaccines encoding HA, NA, or NP also induced protective immune responses in animal models.[24] Intranodal administration of naked NP-encoding mRNA resulted in cross-strain immunity in mice.[25] Intranasal administration of protein-coated chitosan nanoparticles formulated with HA and M2e-encoding mRNAs from H9N2 avian influenza virus induced some protection from H9N2 and H7N9 influenza virus challenge in chickens.[26] Lipid nanoparticle (LNP)-encapsulated nucleoside-modified mRNAs have recently been developed as a vaccine platform, which offers not only exceptional potency, but it is also a rapid, scalable response to viral threats.[27,28] These vaccines have been shown to be effective against a variety of pathogens in preclinical studies,[28] and several clinical studies are underway to prevent viral diseases including those caused by human cytomegalovirus (NCT04232280), respiratory syncytial virus (NCT04528719), severe acute respiratory syndrome-coronavirus 2 (SARS-CoV-2; NCT04470427 and NCT04537949), and others. Importantly, SARS-CoV-2 nucleoside-modified mRNA-LNP vaccines developed by Pfizer-BioNTech and Moderna have proved to be very effective and have received approval for mass vaccination of humans in multiple countries.[29,30] Utilizing this platform, we demonstrated that immunization of mice and ferrets with a single full-length HA-encoding mRNA-LNP induced immune responses against the conserved stalk region of HA, one of the targets of universal influenza virus vaccines.[31] Additionally, we found that elicited immune responses protected mice from homologous, heterologous, and heterosubtypic influenza virus infection. Recent clinical studies by Moderna demonstrated that nucleoside-modified HA mRNA-LNPs are immunogenic and well-tolerated in humans.[32]

Importantly, several studies demonstrated that multiple vaccine antigens could be formulated in mRNA-LNP for delivery in a single immunization,[33–36] and this vaccine platform allows for easy alteration of the antigens they express through modification of the underlying sequence.[37] To improve on influenza virus vaccine targets, we sought to alter protein functional domains by leveraging previously described mutations.

RESULTS

Membrane-anchored HA antigens outperform soluble constructs

Vectored vaccine approaches provide the ability to display antigen in a native, membrane-bound form. We utilized nucleoside-modified mRNA-LNP vaccines expressing influenza virus antigens of interest to study their ability to confer protection from infection. Vaccines were delivered intradermally (I.D.) to mice because I.D. injection has been previously shown to elicit superior responses than intramuscular delivery for this platform in mice.[31] To be consistent with our previous studies and ensure that sufficient responses will be induced, we used 20 μg mRNA-LNP in these experiments.[36] Mice were given only a single shot to mimic the clinical use of influenza virus vaccines, and serological and challenge assays were performed 4 weeks post-vaccination to allow immune responses to develop.

To compare soluble and membrane-bound HA constructs, we designed mRNA sequences that either contained the full-length wild-type A/Michigan/45/2015 H1N1pdm (Mich15) HA sequence or had the transmembrane and cytosolic domains removed and replaced with a T4 foldon trimerization domain (Figure 1A).[38] Further, to examine the effect of HA receptor binding activity on eliciting immune responses, an additional mutation (Y98F) was introduced in the receptor binding site (RBS) to reduce sialic acid binding.[39] Also, mutation of the HA cleavage site (R334A and G335A) was performed to observe whether reduction of proteolytic cleavage plays a role in antigen presentation or stability in the context of intradermal vaccination. Soluble and transmembrane domain-bearing constructs were also produced using the CR #4900 Mini HA, which is based on the conserved stalk domain of the A/Brisbane/59/2007 H1N1 influenza virus.[5] HA-encoding mRNA constructs were analyzed for expression to ensure that secreted and membrane-bound constructs localized to the appropriate positions relative to the cell. Surface staining coupled with flow cytometry analyses of cells transfected with HA antigen-encoding mRNAs revealed that only membrane-bound constructs were detectable on the surface of cells (Figures S1A–S1H). Capture enzyme-linked immunosorbent assays (ELISAs) of transfected cell supernatants were also performed to ensure that secreted antigens were properly expressed (Figure S2A). Membrane-bound antigens were detected at very low levels in these assays, with the exception of membrane-bound Mini HA, implying some amount of leakage for this specific antigen. Next, mice were vaccinated I.D. with 20 μg of a single mRNA-LNP construct and serum was obtained 4 weeks later for analysis (Figure 1B). Sera were analyzed to determine antibody binding by ELISA (Figure 2A; Figure S3A); interference of HA receptor binding activity by hemagglutination inhibition assay (Figure 2B), neutralization by a multi-cycle microneutralization assay (Figure 2C), and antibody Fc-mediated effector functionality through an ADCC reporter assay (Figure 2D; Figure S4A). Mutation of the RBS or the HA cleavage site was not found to substantially impact antigenicity at the tested dose level regardless of whether the antigen was membrane-bound or soluble. However, expression of any HA as a full-length, membrane-bound construct was found to significantly improve the quality of the antibody responses compared with soluble HAs, resulting in more potent

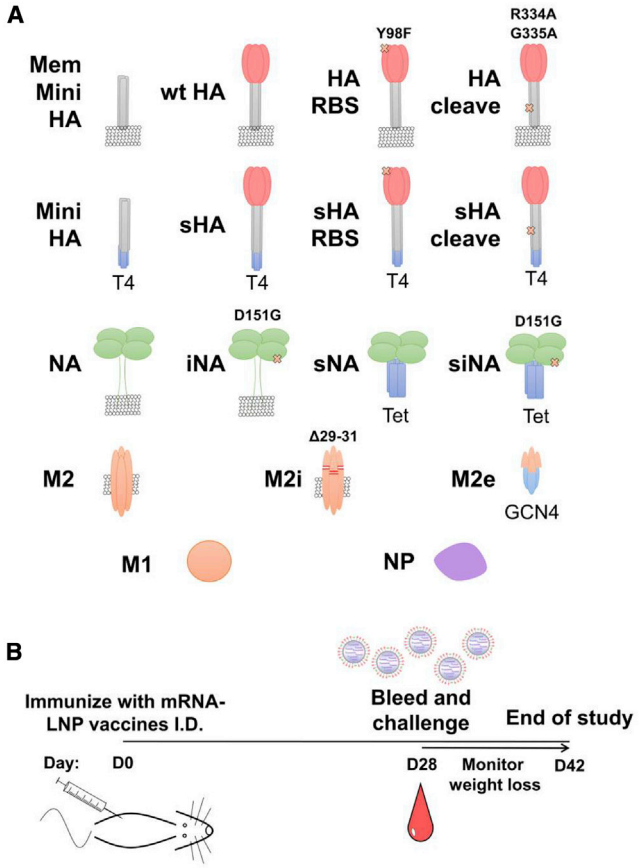

Figure 1. Design of mRNA-encoded influenza virus antigens

(A) Modeled images of the amino acid mutations introduced to each influenza virus vaccine target are illustrated onto their respective protein. Soluble hemagglutinin (sHA) antigens included a T4 foldon trimerization domain (T4) to replace the transmembrane domain and cytoplasmic tail. Soluble neuraminidase (sNA) antigens included a tetrabrachion (Tet) tetramerization domain to replace the stalk and transmembrane domains. The soluble M2 ectodomain (M2e) was fused to a general control non-repressable 4 (GCN4) tetramerization domain. Functional sites were targeted to determine the resulting effect of mutations on conferred immunogenicity for each antigen. Not drawn to scale. (B) Diagram of the vaccination scheme used for comparison of antigen constructs for each individual antigen. Mice were given a single immunization of nucleoside-modified mRNA-LNP vaccine I.D. followed by sera collection 4 weeks later before challenge with influenza virus.

activity in all assays. The responses elicited by Mini HA constructs were overall lower compared to full-length HA and no difference between membrane-bound and secreted Mini HAs was detected. However, these constructs were structurally designed as stable secreted antigens and the impact of introducing a transmembrane domain to these constructs is unclear. Further, it should be noted that the Mini HA is based on the pre-pandemic A/Brisbane/59/2007 H1N1 while all other constructs were based on the post-pandemic Mich15 sequence, which matched the viruses used for these assays.

4 weeks after vaccination, mice were challenged with the pre-pandemic A/New Caledonia/20/1999 H1N1 (NC99) virus to observe

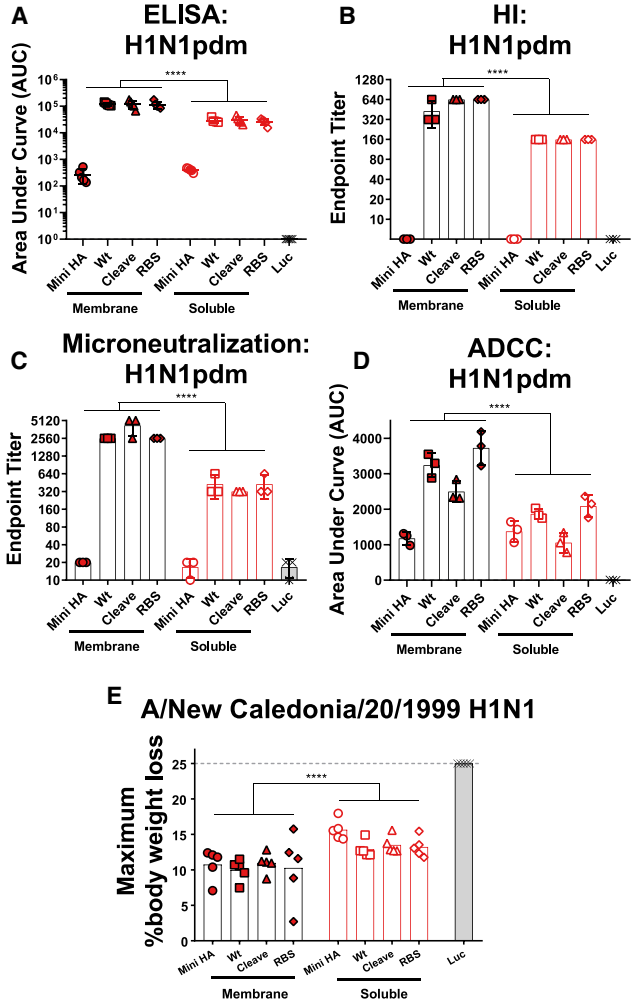

Figure 2. Membrane-bound HA constructs elicit more potent immune responses than soluble forms

Mice were vaccinated with 20 μg of HA-expressing mRNA-LNP vaccines and sera were collected 4 weeks post immunization before challenge with NC99 H1N1 virus. (A) ELISAs were run against purified H1N1pdm virus using sera from individual mice. Data are reported as area under the curve for each sample with group average plus standard deviation (SD; n = 5/group). (B) Hemagglutination inhibition assays were performed against H1N1pdm virus using pooled sera from each group. The assay was run in triplicate with individual values reported as endpoint titers. Bars represent the average of reported values with SD (C) Microneutralization capability of pooled sera was assessed against H1N1pdm influenza virus. Sera were run in triplicate and individual values were reported as endpoint titer, as well as the average plus SD of reported values. (D) Antibody-dependent cell-mediated cytotoxicity reporter assays were performed using H1N1pdm-infected MDCK cells. Pooled sera from each group were run in triplicate and effector cells expressing murine FcγRIV and an NFAT-controlled luciferase reporter were incubated with the infected cells. Data are represented as area under the curve calculated from background-normalized fold change values with the average and SD plotted. (E) Maximum percent body weight loss was calculated after challenge with NC99 and is represented as the average plus individual values for each mouse. Two-way ANOVAs with Tukey's correction for multiple comparisons were performed to determine significance: ****$p < 0.0001$.

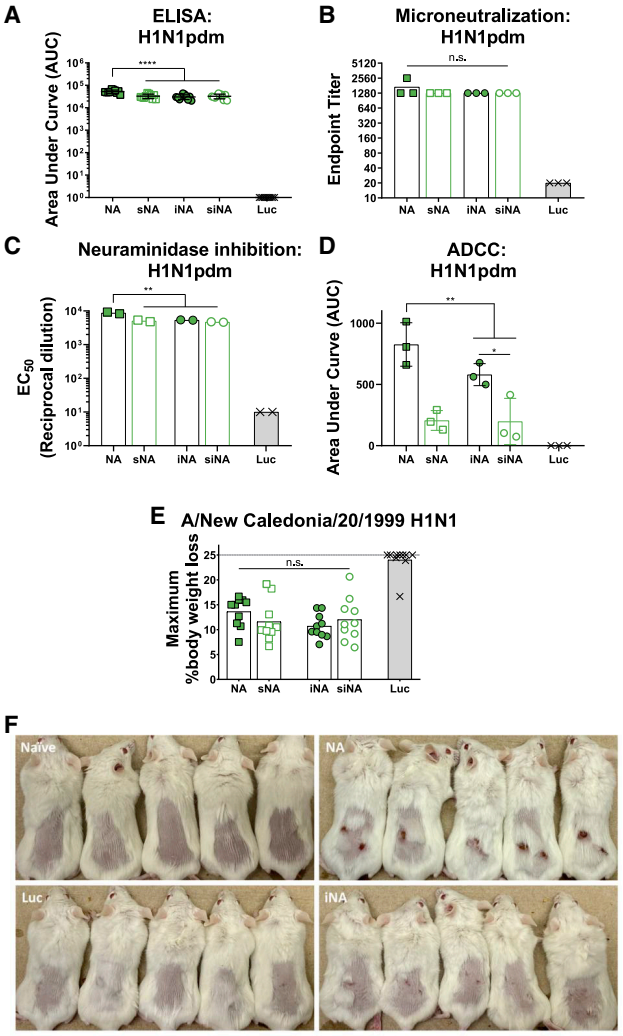

Figure 3. Diminished NA catalytic activity reduces reactogenicity while preserving immunogenicity

Mice were vaccinated and challenged as described in Figure 2. (A) ELISAs of sera from individual mice were run against purified H1N1pdm influenza virus preparations to determine binding titers. Data are reported as area under the curve with the average and SD of values plotted (n = 5/group). (B) Neutralizing potential of sera was determined through a multi-cycle microneutralization assay against H1N1pdm virus. Pooled sera for each group were run in triplicate, and endpoint titers were reported for each replicate. (C) A NA inhibition assay against H1N1pdm virus was performed to examine the ability of sera to block NA catalytic activity. Pooled sera were run in duplicate, and the median effective concentration was reported for each replicate. (D) An ADCC reporter assay was performed on cells infected with H1N1pdm influenza virus. Pooled sera were run in triplicate, and the area under the curve from background normalized fold change values is reported as the average plus SD for each group. (E) Maximum percent body weight loss after heterologous NC99 challenge for each individual mouse is reported (n = 10/group). (F) Mice were vaccinated with 10 μg of mRNA-LNP I.D. in a prime/boost regimen with 3 weeks between administrations. 1 week post boost, mice were photographed to visually examine lesions at the site of vaccination (n = 5/group). Representative images from three independent experiments are shown. One-way ANOVAs with Tukey's correction for multiple comparisons were performed to determine significance: *$p < 0.033$, **$p < 0.002$, ***$p < 0.0002$, ****$p < 0.0001$.

differences in protection conferred by the membrane-bound (Figure S5A) and soluble (Figure S5B) constructs based on body weight loss. Maximum percent body weight loss data demonstrate a significant increase in protection when HA constructs were expressed as full-length membrane-bound protein (Figure 2E). No substantial differences in weight loss were observed for any mutant relative to wild-type antigen, demonstrating a lack of effect of functional mutation for altering HA immunogenicity at the tested dose. It is important to note that the influenza challenge virus NC99 is genetically more similar to the pre-pandemic Mini HA than to the post-pandemic Mich15-based constructs.

Alteration of NA catalytic activity reduces reactogenicity

The impact of mutation of the NA catalytic site was examined by introducing a D151G mutation into the mRNA sequence (iNA, Figure 1A), which has been previously described to reduce functional activity.[40] In parallel, secreted forms of the NA head domain fused to a tetrabrachion tetramerization domain with or without the catalytic site mutant were tested (sNA and siNA, respectively, Figure 1A).[41] Proper expression of membrane-bound and secreted versions of NA constructs was confirmed by *in vitro* cell transfection studies (Figures S1I–S1L, S2B, and S6A). Expression of the wild-type membrane-bound NA, sNA, and siNA were confirmed, but the iNA protein could not be detected by flow cytometry. We could detect a small amount of iNA protein in cell lysates by western blot studies (Figure S6A). Since the iNA construct elicited potent and protective polyclonal antibody responses in immunization studies (see below), we believe that the introduction of the D151G point mutation changes the structure of NA in the binding epitopes of the monoclonal anti-NA antibodies that were used in the *in vitro* experiments, resulting in no (or weak) binding.

Mice were immunized as described above with 20 μg of nucleoside-modified mRNA-LNP, and serological assays were performed 4 weeks after vaccination. All constructs were found to elicit similar levels of antibodies by ELISA to a matched H1N1pdm influenza virus, though wild-type NA elicited slightly stronger responses (Figure 3A; Figure S3B). While neutralizing titers were similar between groups (Figure 3B), NA inhibition measured by an enzyme-linked lectin assay (ELLA) showed again a trend to higher levels for the wild-type construct (Figure 3C). In an ADCC reporter assay, sera from mice immunized with membrane-bound constructs elicited stronger signals (Figure 3D; Figure S4B). To determine the impact of modifications on protection, we infected mice with the heterologous A/New Caledonia/20/1999 H1N1 virus strain. Maximal body weight loss was similar between groups, with no significant differences in protection observed (Figure 3E; Figure S5C).

Interestingly, we observed reactogenicity in the form of lesions when testing the wild-type NA construct in an I.D. prime/boost regimen (10 μg of mRNA-LNP injected twice; 3 weeks apart). The lesions were only observed when testing NA antigens and only after booster vaccination (Figure 3F), suggesting an involvement of adaptive immune responses. Importantly, we found that

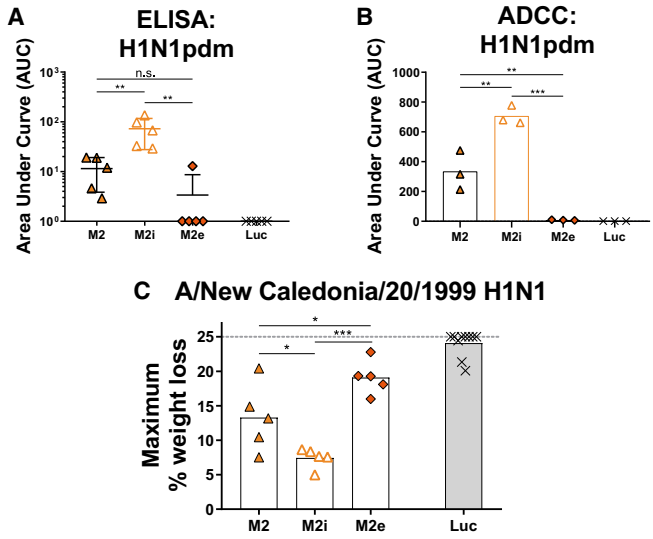

Figure 4. Ablation of full-length matrix protein 2 ion channel activity increases immunogenicity

Mice were vaccinated I.D. with 20 μg of mRNA-LNP expressing M2 constructs. Sera were collected 4 weeks after vaccination followed by challenge with NC99 H1N1 virus. (A) ELISAs were performed using sera from individual mice against purified H1N1pdm virus. Area under the curve was calculated after fitting regression curves to the data and is reported as individual values with average and SD (n = 5/group). (B) ADCC reporter assays were performed to determine effector functionality of antibodies present in sera of immunized mice. Cells were infected with H1N1pdm virus and luminescence was measured as a readout of Fc-receptor engagement. Sera were pooled and run in triplicate for each group. (C) Maximum percent body weight loss from NC99 challenge data is shown as average with each individual point for each animal (n = 5/group). One-way ANOVA with Tukey's correction for multiple comparisons was performed to determine statistical significance: *$p < 0.033$, **$p < 0.002$, ***$p < 0.0002$.

mutating the catalytic site of the NA substantially reduced reactogenicity while the mutation did not substantially alter immunogenicity or conferred protection.

Expression of a full-length M2 with ion channel activity ablated improves immunogenicity

mRNA and other vectored vaccines allow the expression of full-length transmembrane proteins. Comparison of full-length M2 mRNA-LNP with a construct expressing only the M2 ectodomain attached to a general control non-repressible 4 (GCN4) tetramerization domain (M2e) was performed through vaccination followed by serological analysis and challenge.[42] Additionally, a full-length M2-encoding mRNA-LNP with amino acids 29–31 deleted (M2i) was also used (Figure 1A), as this mutation has been previously shown to ablate ion channel activity.[43] Proper expression of M2 and M2i was demonstrated by *in vitro* cell transfection studies (Figures S1M, S1N, S6B, and S6C). Interestingly, we could not detect secreted M2e production *in vitro* (Figures S1O and S6C). One potential explanation for this is that despite being codon-optimized for mammalian cell expression, the M2e construct may work more optimally in bacterial expression systems for which it has been previously developed.[44]

Mice were immunized as described above with 20 μg of nucleoside-modified mRNA-LNP, and serological assays were performed 4 weeks after vaccination. ELISA analysis revealed that M2i-vaccinated mice mounted significantly stronger responses to the target than the other constructs tested (Figure 4A; Figure S3C). This pattern persisted through functional examination of the elicited antibodies by ADCC reporter assays with M2i > M2 > M2e (Figure 4B; Figure S4C). After challenge with the heterologous A/New Caledonia/20/1999 H1N1 strain, protection was examined through analysis of percent body weight loss as described above (Figure S5D). Maximum percent body weight loss was found to be lowest in mice vaccinated with M2i, which showed a significantly higher level of protection than both other vaccine groups (Figure 4C).

NP is a superior antigen to M1 when delivered by nucleoside-modified mRNA-LNP

Internal proteins of the influenza virion have been utilized as targets to stimulate broadly reactive cellular responses through viral vectored approaches.[17,45] To assess the ability of these antigens to confer protection after delivery through an mRNA-LNP, we formulated wild-type NP and M1 (A/Michigan/45/2015 H1N1pdm) expressing vaccines. Vaccination was performed as described above and followed by serological assessment and viral challenge. Modifications to the NP nuclear localization signal sequences to attempt to reduce antibody responses through reduced secretion were also tested but did not translate to differences *in vivo* (Figure S7).

The NP-expressing construct was found to stimulate high levels of antibodies to a purified H1N1pdm target by ELISA, while humoral responses were negligible after vaccination with the M1-expressing mRNA-LNP (Figure 5A; Figure S3D). Survival after viral challenge was complete for both antigens (Figure S5E), but the maximum percent body weight loss was significantly lower in mice receiving NP-expressing mRNA-LNP (Figure 5B).

Analysis of T cell responses was performed for the M1-encoding mRNA-LNP to compare with previously published results on NP-expressing mRNA-LNP vaccination.[36] Mice were vaccinated with 20 μg of M1 mRNA-LNP and spleens were harvested for analysis 12 days later (Figure 5C). T cells were stimulated with M1-specific peptides, and flow cytometry was utilized with intracellular cytokine staining to determine antigen-specific T cell activation. The proportion of cytokine-expressing T cells out of total $CD3^+$ cells is reported for both $CD4^+$ and $CD8^+$ populations (Figures 5D and 5E; Figure S8). Also, polyfunctionality was assessed through Boolean gating to determine cell populations expressing multiple cytokines simultaneously (Figures 5F and 5G). Both $CD4^+$ and $CD8^+$ T cell responses were detected in M1 vaccinated mice. Compared to previously published data for NP-specific T cell responses after mRNA-LNP vaccination,[36] M1-specific $CD8^+$ T cell responses were substantially weaker.

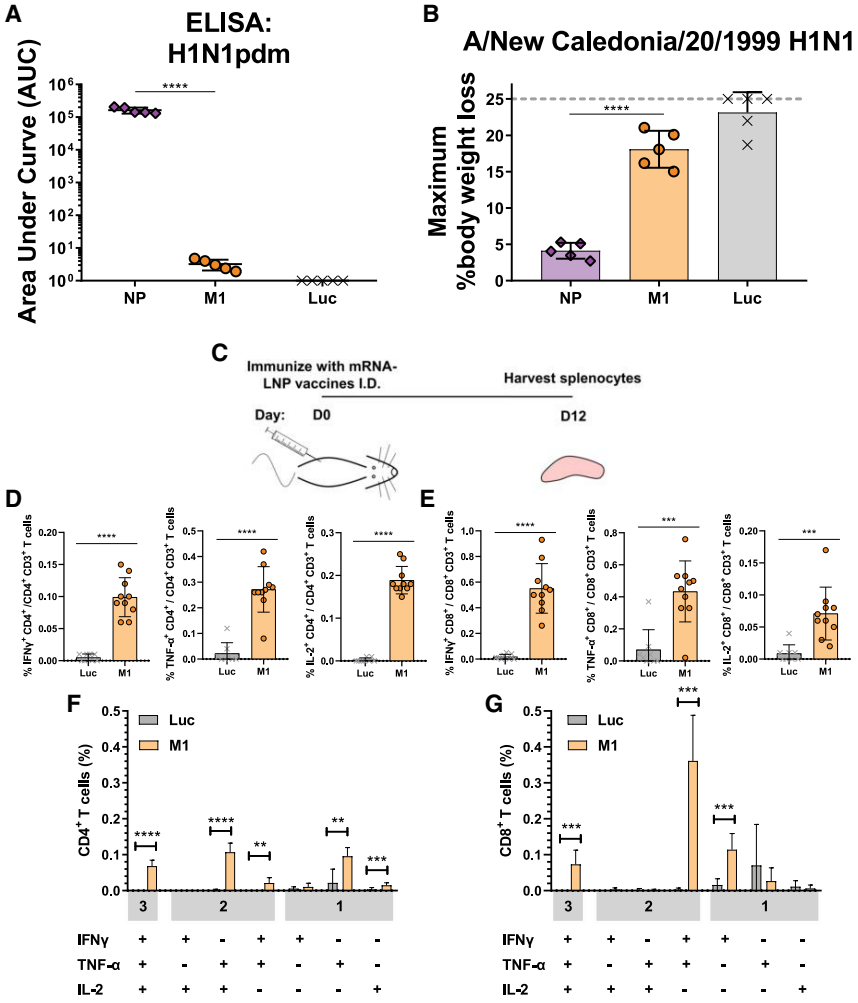

Figure 5. Nucleoside-modified mRNA-LNP delivery of nucleoprotein confers enhanced protection relative to matrix protein 1

Mice were vaccinated with 20 μg nucleoside-modified mRNA-LNP I.D. and bled 4 weeks later for serological analysis before challenge with a heterologous H1N1 virus. (A) ELISA binding titers are displayed as the average area under the curve value and SD for mouse serum sample reactivity to H1N1pdm purified virus (n = 5/group). (B) Maximum percent body weight loss after heterologous NC99 challenge is reported as the average plus SD with each individual value plotted. (C) Mice were vaccinated I.D. with a single dose of 20 μg of M1 mRNA-LNP. Splenocytes were stimulated with an M1 peptide pool 12 days after immunization, and cytokine production by $CD4^+$ and $CD8^+$ T cells was analyzed by flow cytometry. Percentages of M1-specific (D) $CD4^+$ and (E) $CD8^+$ T cells producing IFN-γ, TNF-α, and IL-2 and frequencies of combinations of cytokines produced by (F) $CD4^+$ and (G) $CD8^+$ T cells are shown. Values from M1-immunized mice are compared to values from Luc-immunized animals (B–E). Each symbol represents one animal and error is shown as SD (n = 10 mice/group). Data from two independent experiments are shown (n = 5 mice/group/experiment). (A and B) One-way ANOVA with Tukey's correction for multiple comparisons was performed to determine statistical significance: ****$p < 0.0001$. (D–G) Statistical analysis: paired t test, *$p < 0.05$, **$p < 0.01$, ***$p < 0.001$, ****$p < 0.0001$.

Engineered influenza virus antigen-expressing mRNA-LNPs provide broad protection

To address the breadth of immunity elicited by the above-mentioned vaccine antigens, we performed a challenge study with an influenza virus strain expressing avian H5 and N1 glycoproteins. Mice were vaccinated with 20 μg mRNA-LNP and 4 weeks elapsed between vaccination and challenge with a lethal dose of a recombinant influenza virus strain expressing A/Vietnam/1204/2004 H5N1 glycoproteins with the HA poly-basic cleavage site removed. Weight loss was monitored for 14 days (Figure S9) with maximum percent weight loss reported for each mouse (Figure S10). Protection was observed for mice vaccinated with influenza virus antigens, with similar patterns to those seen for NC99 challenge (membrane-bound HA performed better than soluble HA, NA performance was similar across groups, and M2 and M2i protected well while M2e did not). To further explore the breadth of antibody binding responses induced by various mRNA-encoded influenza antigens, we performed ELISAs using serum from immunized mice 4 weeks post vaccination. Binding to a diverse panel of influenza virus strains representative of pre-pandemic H1N1, H5N1, H3N2, and influenza B subtypes was investigated (Figure S11). Binding titers were found to extend to the avian H5N1 virus, but not to the group 2 HA and NA expressing H3N2 virus. Little reactivity was observed against the influenza virus B strain tested. These binding patterns are consistent with the patterns of cross-reactivity previously described for influenza viruses.[46]

DISCUSSION

Antigen modification of vaccines has been commonly used to increase stability/immunogenicity of recombinantly expressed protein antigens.[47] Expanding this process to include alteration of functional domains has been explored to determine the specific effects modifications have on immunogenicity and reactogenicity.[47] Due to its synthetic nature, the nucleoside-modified mRNA-LNP technology enables the rapid incorporations of changes to the protein target through modification of the underlying sequence. We applied this procedure to potentially broadly protective influenza virus vaccine antigens in an attempt to optimize each component.

We found that vaccination with full-length HA with the intact transmembrane region elicited more functional and protective antibody responses than soluble constructs when delivered by nucleoside-modified mRNA-LNP. This is likely due to increased stabilization

of the HA protein through this native domain rather than a foreign soluble trimerization domain. Furthermore, accumulation of membrane-bound antigen on the cell surface may facilitate more effective cross-linking of B cell receptors, resulting in stronger antibody responses. This beneficial effect may be transferred to secreted antigens by polymerization through presentation on nanoparticles such as ferritin.[7] Mutation of the HA RBS or cleavage site had little impact on immunogenicity in either secreted or membrane-bound form. The Mini HA antigen also benefited from regrafting of the transmembrane domain as protection conferred was similar to the wild-type antigen after heterologous challenge. The observed protective effect was similar for all constructs, but it is important to note that the Mini HA was closer in amino acid sequence to the pre-pandemic NC99 challenge virus than the post-pandemic Mich15-based constructs. Based on the decreased activity of sera from Mini HA-vaccinated mice *in vitro*, it is likely that the full-length antigens would result in superior protection against challenge with matched strains.

Modification of the NA revealed little impact of diminished catalytic activity on immunogenicity of the antigen. Some advantage was seen for the wild-type antigen in binding and functional assays, but the conferred protection by all tested antigens was similar. ADCC activity was most affected by antigen modification, with full-length constructs showing an increase in reporter activity relative to their secreted counterparts. This result could imply that epitopes targeted by antibodies that mediate ADCC activity are lost when the entire stalk domain is removed to design the soluble constructs. Interestingly, we found that reactogenicity was substantially decreased when catalytic activity of the antigen was reduced. This result could be due to effects of the NA to activate cytokines such as transforming growth factor-β or through direct desialylation of Toll-like receptors, which can stimulate inflammatory signaling.[48,49] This response only occurred during vaccine boosting, which implies that some function of the adaptive immune response is at play to cause this reactogenicity, potentially the reactivity of tissue-resident memory T cells. Discovery of this reactogenicity has not been previously reported, which could be due to the intradermal route of administration that allows for easy visualization of lesion formation. This finding could be broadly applicable to improve safety of NA-based vaccines for a variety of platforms and could be more generally applied to antigens with enzymatic activity.

Analysis of M2 constructs revealed the benefit of preserving the entire transmembrane domain, which contains T cell epitopes and is involved in presenting the appropriately folded conformation of the antigen to the cell surface. Ablation of ion channel activity increased stimulated immune responses, most likely due to a decrease in toxicity that overexpression of active ion channels on the cell surface would impart. Expression of the soluble M2e construct showed poor immunogenicity in the context of delivery by mRNA-LNP, which could be due to lack of appropriate conformation when expressed *in vivo*, or limited B cell receptor cross-linking in the context of a small, secreted antigen. The antigen is typically expressed in a bacterial system and highly purified to only maintain correctly folded tetrameric constructs.[16] The lack of this quality control *in vivo* could lead to expression of a majority of misfolded or inappropriate antigens, which could prevent an optimal response. Also, delivering this antigen in a prime-boost regimen may increase its potency.

Comparison of internal proteins previously selected for viral vectored vaccines revealed the benefit of delivery of NP by mRNA-LNP over M1. The level of protection conferred by NP was significantly higher than that seen through delivery of M1, and comparison with previous data showed that the stimulation of $CD8^+$ T cells is much greater after exposure to NP. Antibody responses to these antigens were significantly different, with potent antibody responses observed against NP and with little to no M1 response detected. This result corroborates previous studies that found a low seroprevalence of M1-specific responses in the general population, which suggests that M1 is a poor B cell target.[50] Functionality of NP-specific antibodies has been debated in the field, but the combination of these responses with a potent T cell response has potentially led to effective protection from influenza virus challenge in a murine model.

In summary, modification of antigens has been shown to change immunogenicity and reactogenicity of universal influenza virus vaccine targets utilizing the nucleoside-modified mRNA-LNP vaccine platform. The dose of vaccination used in this study leads to high amounts of antigen expressed for each individual construct, which could have overwhelmed some of the subtle effects that mutation could have had on immunogenicity if lower doses were utilized. Some of the findings in this study may broadly apply to other vaccine platforms and viral antigens. Structure-guided approaches to rational vaccine design tend to focus on stabilization of antigens or presentation of specific epitopes.[47] Combining these efforts with modification of functional domains could lead to improved antigen characteristics, which may benefit general vaccine development.

MATERIALS AND METHODS

Ethics statement

The investigators faithfully adhered to the "Guide for the Care and Use of Laboratory Animals" by the Committee on Care of Laboratory Animal Resources Commission on Life Sciences, National Research Council. Mouse studies were conducted under protocols approved by the Institutional Animal Care and Use Committees (IACUC) of the University of Pennsylvania (UPenn) and the Icahn School of Medicine at Mount Sinai (ISMMS). All animals were housed and cared for according to local, state, and federal policies in an Association for Assessment and Accreditation of Laboratory Animal Care International (AAALAC)-accredited facility.

Viruses, cells, and proteins

Influenza A viruses A/Michigan/45/2015 H1N1pdm (Mich15), A/New Caledonia/20/1999 H1N1 (NC99), and IVR-180 (HA and NA from A/Singapore/GP1908/2015 H1N1pdm virus and non-glycoproteins from A/Texas/1/1977 H3N2) were utilized in this study. Viruses were grown in 10-day-old embryonated chicken eggs (Charles River) for 48 h at 37°C before placing at 4°C overnight.

Allantoic fluid was harvested and cleared of debris through centrifugation at 4,000 × *g* for 10 min at 4°C. Cleared allantoic fluid, which was found to be hemagglutination positive (described below), was pooled, aliquoted, and stored at −80°C until use. To purify and concentrate virus, we centrifuged pooled allantoic fluid at 100,000 × *g* for 2 h at 4°C over a 30% sucrose cushion. Viral pellets were resuspended in phosphate buffered saline (PBS), protein concentration was measured using a Bradford assay, and aliquots were frozen at −80°C until use.

Madin-Darby canine kidney (MDCK) cells were grown in complete Dulbecco's modified Eagle's medium (DMEM; 10% FBS [GIBCO], 100 units/mL penicillin, and 100 μg/mL streptomycin [GIBCO], and 1 mM 4-[2-hydroxyethyl]-1-piperazineethanesulfonic acid [HEPES; GIBCO]) at 37°C and 5% CO_2. Neuro-2a cells (ATCC) were cultured in DMEM + GlutaMAX (GIBCO), 10% FBS (Gemini Bio), and 100 units/mL penicillin and 100 μg/mL streptomycin (Invitrogen).

mRNA production

A/Michigan/45/2015 H1N1pdm virus segment sequences were utilized for antigen design. Codon-optimized HA, NA, NP, M1, and M2 were synthesized (Genscript) and mutations were included in the nucleotide sequence through polymerase chain reaction-guided amplification. Constructs were ligated into mRNA production vectors, vectors were linearized, and a T7-driven *in vitro* transcription reaction (Megascript, Ambion) was performed to generate mRNA with 101 nucleotide long poly(A) tails. Capping of mRNA was performed in concert with transcription through addition of a trinucleotide cap1 analog, CleanCap (TriLink), and m1Ψ-5′-triphosphate (TriLink) was incorporated into the reaction instead of UTP. Cellulose-based purification of mRNA was performed as described.[51] mRNAs were then checked on an agarose gel before storing at −20°C.

Lipid nanoparticle formulation of mRNA

Purified mRNAs were lipid nanoparticle formulated using a self-assembling ethanolic lipid mixture of an ionizable cationic lipid, phosphatidylcholine, cholesterol, and polyethylene glycol-lipid. This mixture was rapidly combined with an aqueous solution containing mRNA at acidic pH as previously described.[27] The ionizable cationic lipid (pKa in the range of 6.0–6.5, proprietary to Acuitas Therapeutics) and LNP composition are described in the patent application WO 2017/004143. The average hydrodynamic diameter was ∼80 nm with a polydispersity index of 0.02–0.06 as measured by dynamic light scattering using a Zetasizer Nano ZS (Malvern Instruments, Malvern, UK) and an encapsulation efficiency of ∼95% as determined using a Ribogreen assay.

mRNA transfection

Transfection of Neuro-2a cells was performed utilizing TransIT-mRNA (Mirus Bio), according to the manufacturer's instructions: mRNA (0.1 μg) was combined with TransIT-mRNA Reagent and Boost Reagent in 17 μL serum-free medium, and the complex was added to 3×10^4 cells in 183 μL complete medium. After overnight incubation at 37°C, supernatant was collected, and mRNA-transfected cells were lysed for 30 min on ice in radioimmunoprecipitation assay (RIPA) buffer (Sigma). Cells analyzed by flow cytometry were not treated but instead only harvested and subsequently stained.

Staining and flow cytometric analyses of mRNA-transfected neuro-2a cells

1.2×10^5 transfected cells were washed twice with and resuspended in fluorescence-activated cell sorting (FACS) buffer (2% FBS in PBS). Cells were then incubated on ice for 20 min with 7.5 μg/mL of anti-HA (CR9114) or anti-NA (1G01) human monoclonal antibodies or anti-M2 (E10) mouse monoclonal antibody and washed again with FACS buffer. Finally, cells were incubated on ice for 20 min with either a 1:300 dilution of goat anti-human immunoglobulin G (IgG; H+L) Alexa Fluor 647 (Invitrogen) or a 1:900 dilution of goat anti-mouse (IgG+IgM) fluorescein isothiocyanate (FITC; Cayman Chemical). The presence of AF647 or FITC-labeled antibody on cell surfaces was detected on a BD LSRII flow cytometer. At least 50,000 events for each sample were recorded and data were analyzed with the FlowJo 10 software.

Western blot analysis

Western blots were performed on transfected Neuro 2a cell lysates. 15 μL (4.5×10^4 cells) of cell lysate was diluted in 2× Laemmli buffer (BioRad) containing β-mercaptoethanol and boiled for 5 min. Samples were run on a 4%–20% gradient Mini Protean TGX gel (BioRad) for sodium dodecyl sulfide polyacrylamide gel electrophoresis. Novex Sharp Prestained Color Protein standard was used as a protein size marker. After running, proteins were transferred to a 0.2 μm polyvinylidene difluoride (PVDF) membrane using a TransBlot Turbo Transfer Pack (BioRad). Blots were rinsed with PBST and blocked with 3% milk in PBST for 1 h at room temperature (RT), shaking. Primary antibody was diluted in 1% milk in PBST (1 μg/mL E10; 1.37 μg/mL 4A5; 1:20,000 anti-GAPDH [Millipore Sigma]) and added to blots before shaking overnight at 4°C. Blots were washed 3 times with PBST for 5 min each. Secondary antibody (goat anti-mouse IgG Fc; Abcam) was diluted 1:5,000 in 1% milk, and blots were incubated at RT for 1 h shaking. Blots were washed 3 times with PBST for 5 min, developed with a Pierce ECL Western Blotting substrate (Thermo Scientific), and imaged using a ChemiDoc XRS+ machine (BioRad).

mRNA vaccination and viral challenge

Female BALB/c mice aged 6 to 8 weeks (Jackson Labs-ISMMS and Charles River Laboratories-UPenn) were utilized for this study. Mice were anesthetized with a low dose of ketamine/xylazine mixture (ISMMS) or isoflurane (UPenn) and shaved before intradermal delivery of mRNA-LNP vaccine diluted in PBS in two different spots on the back to a total volume of 100 μL.

The influenza virus challenge dose was determined through infection of mice with log-fold decreasing plaque-forming units of virus. The median lethal dose (LD_{50}) was calculated based on survival of mice

and the dose received, and a challenge dose of 5 × LD_{50} was calculated. At the time of challenge, mice were anesthetized with a ketamine/xylazine mixture and weighed before 5 × LD_{50} of influenza virus was administered intranasally in 50 μL of PBS. Mice were weighed daily and were sacrificed if weight loss was greater than 25% of initial body weight or at the experiment end.

ELISA

In vitro studies (capture ELISA)

Immulon 4 HBX flat-bottomed, 96-well plates (Thermo Fisher) were coated with 2 μg/mL of antibody in PBS overnight at 4°C (100 μL/well). Detection antibodies were biotinylated with EZ-Link NHS-PEG4-Biotin, No Weigh Format (Thermo Fisher), incubated at RT for 30 min and buffer exchanged into PBS using Zeba desalting columns (Thermo Fisher). Plates were blocked for 1 h at RT in 3% goat serum (GIBCO) and 0.25% milk (Quality Biological) in PBST. Cell culture supernatant was incubated 1:1 (125 μL lysate: 125 μL zwittergent) with 0.05% zwittergent 3-14 (Millipore sigma) in PBST for 1 h at RT. A/Michigan/45/2015 pH1N1 virus used as positive control and was diluted 1:10 in 0.05% zwittergent 13-4 (final concentration 63 μg/mL). Blocking buffer was removed and cell lysates were serially diluted 1:2 in blocking buffer and incubated for 2 h at RT. After washing three times with PBST, detection antibody was added at 100 μL/well at 5 μg/mL and incubated for 1 h at RT. Plates were again washed three times with PBST and streptavadin-horseradish peroxidase (HRP; Pierce) was diluted 1:3,000 in blocking buffer and added at 100 μL/well and incubated for 1 h at RT. Plates were washed four times with PBST and developed using 100 μL of Sigma OPD (Sigma) for 10 min before quenching with 3M HCl (Fisher). Plates were read on a Synergy H1 hybrid multimode microplate reader (BioTek) at 490 nm. Data were processed using Prism 8.0 (GraphPad) and area under the curve was calculated using a baseline of the average plus three times the standard deviation of negative wells or 0.07, whichever value was higher.

Analyses of serum samples from mouse immunization studies

Immulon 4 HBX flat-bottomed, 96-well plates (Thermo Fisher) were coated with purified virus in PBS at a final concentration of 250 ng per well and allowed to incubate overnight at 4°C. The following morning, plates were washed three times with 0.1% Tween 20 (Fisher) in PBS (PBST) and blocked in Blocking Buffer (3% goat serum [GIBCO] and 0.25% milk [Quality Biological] in PBST) for 1 h at RT. After removal of Blocking Buffer, serum samples were serially diluted 3-fold in fresh Blocking Buffer and allowed to incubate at RT for 2 h. Plates were then washed three times with PBST and goat anti-mouse IgG Fc HRP-linked secondary antibody (Abcam, 97265) was added at a concentration of 1:15,000 in Blocking Buffer and incubated at RT for 1 h. Plates were then washed four times with PBST with additional shaking and developed using SigmaFast o-phenylenediamine dihydrochloride substrate (OPD; Sigma) for 10 min before quenching with 3M HCl (Fisher). Plates were read on a Synergy H1 hybrid multimode microplate reader (BioTek) at 490 nm. Data were processed using Prism 8.0 (GraphPad), and area under the curve was calculated using a baseline of the average plus three times the standard deviation of negative wells or 0.07, whichever value was higher.

Hemagglutination inhibition assay

Hemagglutination titer was determined through incubation of 2-fold serial dilutions of virus in PBS with an equal volume of chicken red blood cells (RBCs) at 0.5% in PBS at 4°C. Titer was determined as the final dilution able to cause agglutination of RBCs, which prevents a pellet from being formed.

Serum was treated with receptor destroying enzyme (RDE; Seiken) as per the manufacturer's instruction. Briefly, serum was incubated with RDE overnight at 37°C and then the reaction was quenched with 2.5% sodium citrate (Fisher), heat inactivated at 56°C for 30 min, and diluted to a final concentration of 1:10 in PBS. Serum was then serially diluted 2-fold in PBS. Virus was diluted to four hemagglutination units in PBS and added to serum dilutions. The mixture was shaken for 30 min at RT then added to chicken RBCs at 0.5% in PBS and allowed to develop at 4°C. Endpoint titer was determined as the final reciprocal dilution able to prevent agglutination of RBCs, denoted visually by pelleted RBCs.

Microneutralization assay

Median tissue culture infectious dose ($TCID_{50}$) was determined for each virus utilized in this assay. MDCK cells were plated at 2.5 × 10^4 cells per well in tissue culture-treated 96-well dishes and allowed to culture overnight at 37°C and 5% CO_2. The following morning, virus was serially diluted in half-log increments in assay buffer (Ultra MDCK media [Lonza] with 1 μg/mL 6-[1-tosylamido-2-phenyl] ethyl chloromethyl ketone [TPCK]-treated trypsin). Cells were washed with PBS and infected with viral dilutions for 72 h at 33°C. A hemagglutination assay was performed by mixing 50 μL of supernatant from each well with 50 μL of 0.5% chicken RBCs (Lampire). The last dilution, which was able to cause agglutination of RBCs was recorded and used to calculate $TCID_{50}$.

MDCK cells were plated in 96-well dishes at 2.5 × 10^4 cells/well. Serum samples were pooled and RDE treated as described above. Sera were then diluted 2-fold in assay buffer before adding equal volumes of diluted sera with 100 $TCID_{50}$ of influenza virus diluted in assay buffer. This mixture was shaken at RT for 30 min before adding to PBS-washed MDCK cells and allowing virus to adsorb for 1 h at 33°C and 5% CO_2. Cells were washed with PBS and remaining sera were diluted in an equal volume assay buffer before adding to the corresponding wells. Infection was allowed to proceed before reading of the plate via hemagglutination assay. The last dilution that was able to cause agglutination of RBCs was determined as the endpoint titer.

ADCC reporter assay

MDCK cells were plated in white-walled, 96-well dishes (CoStar) to 2.5 × 10^4 cells/well in cDMEM and incubated overnight at 37°C and 5% CO_2. The following morning, cells were washed with PBS and infected with influenza virus at a multiplicity of infection of five in the absence of TPCK-treated trypsin. Infection was allowed

to proceed for 24 h at 37°C and 5% CO_2. Media were removed from cells and 25 μL of assay buffer (RPMI 1640 with 4% Low IgG FBS [GIBCO]) was added to each well. Serum was diluted 25-fold then serially diluted in 3-fold steps in assay buffer and 25 μL was added to the infected cells. Effector ADCC cells expressing murine FcγRIV with an NFAT-driven luciferase cassette (Promega) were added to a final count of 3×10^6 cells/mL in 25 μL. The reaction was allowed to incubate for 6 h at 37°C and 5% CO_2 before normalizing to RT. Bio-Glo luciferase substrate (Promega) was added to each well and luminescence was immediately read with a Synergy H1 hybrid multimode microplate reader (BioTek). Fold change was determined by dividing each well by the average of background wells plus three times the standard deviation. Regression curves were fit to the background corrected values and area under the curve was calculated with a baseline threshold of one in Prism 8.0 (GraphPad).

NA inhibition assay

ELLAs were performed to determine the amount of virus necessary for neuraminidase inhibition assays. Fetuin (Sigma-Aldrich) was coated in 96-well dishes at a final concentration of 25 μg/mL in 100 μL PBS and plates were stored overnight at 4°C. The following day, plates were washed three times with PBST and blocked with 5% BSA in PBST for 1 h at RT. Virus was serially diluted 2-fold in PBS with 1% BSA (Sigma-Aldrich) and added to blocked plates for 2 h at 37°C and 5% CO_2. Plates were then washed six times with PBST, 100 μL of HRP-conjugated peanut agglutinin (PNA) at 5 μg/mL was added, and plates were incubated for 2 h at RT in the dark. After washing six times with PBST, 100 μL of SigmaFast OPD (Sigma) was added and allowed to develop for 10 min before quenching with 3M HCl (Fisher). Plates were read on a Synergy H1 hybrid multimode microplate reader (BioTek) at 490 nm. Curves were fit using non-linear regression in Prism 8.0 (GraphPad) and the 90% effective concentration (EC_{90}) was determined and used for subsequent NA inhibition assays.

96-well dishes were coated with 25 μg/mL fetuin in 100 μL PBS and stored overnight at 4°C. Sera were heat-treated at 56°C and diluted 1:30 before diluting 2-fold in PBS with 1% BSA. Virus was diluted in PBS with 1% BSA based on the pre-determined EC_{90} value and was added in equal volumes to the serum dilutions and incubated, shaking at RT for 1.5 h. Fetuin-coated plates were washed and blocked for 1 h at RT as described above. After removing blocking buffer, virus/serum mixture was added to the fetuin plates and incubated at 37°C and 5% CO_2 for 2 h. Plates were then washed six times with PBST and HRP-linked PNA was added for 2 h at RT in the dark. Plates were washed again six times with PBST and developed as described above. Nonlinear regression curves were fit using Prism 8.0 (GraphPad) and EC_{50} values were determined.

Staining and flow cytometry analysis of mouse splenocytes

Single-cell suspensions of mouse splenocytes were generated in complete RPMI-1640 medium. 3×10^6 cells per sample were stimulated for 6 h at 37°C and 5% CO_2 in the presence of an overlapping M1 peptide pool (JPT Peptide Technologies, MP1/California H1N1) at 5 μg/mL and anti-CD28 antibody (BD Biosciences, clone 37.51) at 1 μg/mL. GolgiPlug (BD Biosciences, Brefeldin A) at 5 μg/mL and GolgiStop (BD Biosciences, Monensin) at 10 μg/mL were added to each sample 1 h after the start of stimulation. Unstimulated samples for each animal were also included. A sample stimulated with phorbol 12-myristate-13-acetate (Sigma) at 10 μg/mL and ionomycin (Sigma) at 200 ng/mL was included as a positive control. After stimulation, cells were washed with PBS and stained with a LIVE/DEAD Fixable Aqua Dead Cell Stain Kit (Life Technologies) for 10 min in the dark at RT. Cells were subsequently surface stained with unlabeled CD16/CD32 rat anti-mouse (BD Biosciences, clone 2.4G2) and anti-CD4 PerCP (peridinin chlorophyll protein)/Cy5.5 (BioLegend, clone GK1.5) and anti-CD8 Pacific Blue (BioLegend, clone 53-6.7) monoclonal antibodies (mAbs) for 30 min in the dark at 4°C. After surface staining, cells were washed with FACS buffer, fixed (PBS containing 1% paraformaldehyde), and permeabilized using a Permeabilization/Fixation Solution Kit (BD Biosciences). Cells were then intracellularly stained with anti-CD3 allophycocyanin (APC)-Cy7 (BD Biosciences, clone 145-2C11), anti-tumor necrosis factor-α (TNF-α) phycoerythrin (PE)-Cy7 (BD Biosciences, clone MP6-XT22), anti-interferon-γ (IFN-γ) Alexa Fluor 700 (AF700; BD Biosciences, clone XMG1.2), and anti-interleukin-2 (IL-2) Brilliant Violet 711 (BV711; BioLegend, clone JES6-5H4) mAbs for 30 min in the dark at 4°C. Finally, cells were washed with permeabilization buffer, fixed as before, and stored at 4°C until analysis. Splenocytes were analyzed on a modified LSR II flow cytometer (BD Biosciences). 500,000 events were collected per specimen. After the gates for each function were developed, the Boolean gate platform was used to create the full array of possible combinations, equating to seven response patterns when testing three functions. Data was analyzed with the FlowJo 10 program. Data were expressed by subtracting frequencies of unstimulated stained cells from frequencies of peptide pool-stimulated stained samples.

Statistical analyses

Data were analyzed for statistical significance using Prism 8.0 (GraphPad). For datasets with multiple independent variables, two-way ANOVAs with Tukey's correction for multiple comparisons was utilized. One-way ANOVAs with Tukey's correction for multiple comparisons were performed on datasets where a single independent variable was being measured.

SUPPLEMENTAL INFORMATION

Supplemental information can be found online at https://doi.org/10.1016/j.omtm.2021.06.003.

ACKNOWLEDGMENTS

We would like to thank Michael Schotsaert and Angela Choi for sharing the NC99 challenge virus. The study was partially supported by NIH R01-AI146101 (N.P. and R.N.), National Institute of Allergy and Infectious Disease (NIAID) Collaborative Influenza Vaccine Innovation Centers (CIVIC) contract 75N93019C00051 (F.K., R.N., and P.P.), a Public Health Service Institutional Research Training Award AI07647 (AWF), NIH grant 5P01AI097092 - *Toward a*

Universal Influenza Virus Vaccine (P.P.), the Center of Excellence in Influenza Research and Surveillance (CEIRS) contract HHSN272201400008C (P.P.), and NIH grant R01AI145870 (P.P.).

AUTHOR CONTRIBUTIONS

N.P., R.N., and A.W.F. conceived the study. N.P., R.N., A.W.F., M.P., and M. Benz designed experiments. N.P., R.N., A.W.F., and H.M. designed mRNA sequences. N.P. and H.M. produced antigen-encoding mRNA. A.W.F., M.P., V.C.R., M. Benz, M.M., and R.N. performed experiments. N.P., R.N., A.W.F., M.P., M. Benz, F.K., and P.P. reviewed and interpreted data. Y.K.T. and M. Beattie designed and produced the LNP vaccines. A.W.F. drafted and all authors contributed to the preparation of the manuscript. All authors had full access to the data and gave final approval before submission.

DECLARATION OF INTERESTS

The Icahn School of Medicine has filed patents on influenza virus vaccines, naming R.N., F.K., and P.P. as inventors. In accordance with the University of Pennsylvania policies and procedures and our ethical obligations as researchers, we report that N.P. and Y.K.T. are named on a patent describing the use of nucleoside-modified mRNA in lipid nanoparticles as a vaccine platform. N.P., R.N., P.P., F.K., and A.W.F. are named on a patent filed on universal influenza vaccines using nucleoside-modified mRNA. We have disclosed those interests fully to the University of Pennsylvania and The Icahn School of Medicine at Mount Sinai, and we have in place an approved plan for managing any potential conflicts arising from licensing of our patents. M. Beattie and Y.K.T. are employees of Acuitas Therapeutics, a company focused on the development of LNP nucleic acid delivery systems for therapeutic applications.

REFERENCES

1. WHO (2020). Influenza (Seasonal) Fact Sheet, https://www.who.int/news-room/fact-sheets/detail/influenza-(seasonal.
2. CDC (2019). Seasonal Influenza Vaccine Effectiveness, 2004-2019, https://www.cdc.gov/flu/vaccines-work/effectiveness-studies.htm.
3. Nachbagauer, R., and Palese, P. (2020). Is a Universal Influenza Virus Vaccine Possible? Annu. Rev. Med. *71*, 315–327.
4. Bernstein, D.I., Guptill, J., Naficy, A., Nachbagauer, R., Berlanda-Scorza, F., Feser, J., Wilson, P.C., Solórzano, A., Van der Wielen, M., Walter, E.B., et al. (2020). Immunogenicity of chimeric haemagglutinin-based, universal influenza virus vaccine candidates: interim results of a randomised, placebo-controlled, phase 1 clinical trial. Lancet Infect. Dis. *20*, 80–91.
5. Impagliazzo, A., Milder, F., Kuipers, H., Wagner, M.V., Zhu, X., Hoffman, R.M., van Meersbergen, R., Huizingh, J., Wanningen, P., Verspuij, J., et al. (2015). A stable trimeric influenza hemagglutinin stem as a broadly protective immunogen. Science *349*, 1301–1306.
6. Widge, A.T. (2019). Dose, safety, tolerability and immunogenicity of an influenza H1 stabilized stem ferritin vaccine, VRCFLUNPF099-00-VP, in healthy adults. ClinicalTrials.gov., NCT03814720.
7. Yassine, H.M., Boyington, J.C., McTamney, P.M., Wei, C.J., Kanekiyo, M., Kong, W.P., Gallagher, J.R., Wang, L., Zhang, Y., Joyce, M.G., et al. (2015). Hemagglutinin-stem nanoparticles generate heterosubtypic influenza protection. Nat. Med. *21*, 1065–1070.
8. DiLillo, D.J., Tan, G.S., Palese, P., and Ravetch, J.V. (2014). Broadly neutralizing hemagglutinin stalk-specific antibodies require FcγR interactions for protection against influenza virus in vivo. Nat. Med. *20*, 143–151.
9. Eggink, D., Goff, P.H., and Palese, P. (2014). Guiding the immune response against influenza virus hemagglutinin toward the conserved stalk domain by hyperglycosylation of the globular head domain. J. Virol. *88*, 699–704.
10. Bajic, G., Maron, M.J., Adachi, Y., Onodera, T., McCarthy, K.R., McGee, C.E., Sempowski, G.D., Takahashi, Y., Kelsoe, G., Kuraoka, M., and Schmidt, A.G. (2019). Influenza Antigen Engineering Focuses Immune Responses to a Subdominant but Broadly Protective Viral Epitope. Cell Host Microbe *25*, 827–835.e6.
11. Wohlbold, T.J., Nachbagauer, R., Xu, H., Tan, G.S., Hirsh, A., Brokstad, K.A., Cox, R.J., Palese, P., and Krammer, F. (2015). Vaccination with adjuvanted recombinant neuraminidase induces broad heterologous, but not heterosubtypic, cross-protection against influenza virus infection in mice. MBio *6*, e02556.
12. Stadlbauer, D., Zhu, X., McMahon, M., Turner, J.S., Wohlbold, T.J., Schmitz, A.J., Strohmeier, S., Yu, W., Nachbagauer, R., Mudd, P.A., et al. (2019). Broadly protective human antibodies that target the active site of influenza virus neuraminidase. Science *366*, 499–504.
13. Krammer, F., Fouchier, R.A.M., Eichelberger, M.C., Webby, R.J., Shaw-Saliba, K., Wan, H., Wilson, P.C., Compans, R.W., Skountzou, I., and Monto, A.S. (2018). NAction! How Can Neuraminidase-Based Immunity Contribute to Better Influenza Virus Vaccines? MBio *9*, e02332-17.
14. Deng, L., Cho, K.J., Fiers, W., and Saelens, X. (2015). M2e-Based Universal Influenza A Vaccines. Vaccines (Basel) *3*, 105–136.
15. El Bakkouri, K., Descamps, F., De Filette, M., Smet, A., Festjens, E., Birkett, A., Van Rooijen, N., Verbeek, S., Fiers, W., and Saelens, X. (2011). Universal vaccine based on ectodomain of matrix protein 2 of influenza A: Fc receptors and alveolar macrophages mediate protection. J. Immunol. *186*, 1022–1031.
16. Schotsaert, M., Ysenbaert, T., Smet, A., Schepens, B., Vanderschaeghe, D., Stegalkina, S., Vogel, T.U., Callewaert, N., Fiers, W., and Saelens, X. (2016). Long-Lasting Cross-Protection Against Influenza A by Neuraminidase and M2e-based immunization strategies. Sci. Rep. *6*, 24402.
17. Berthoud, T.K., Hamill, M., Lillie, P.J., Hwenda, L., Collins, K.A., Ewer, K.J., Milicic, A., Poyntz, H.C., Lambe, T., Fletcher, H.A., et al. (2011). Potent CD8+ T-cell immunogenicity in humans of a novel heterosubtypic influenza A vaccine, MVA-NP+M1. Clin. Infect. Dis. *52*, 1–7.
18. Topham, D.J., Tripp, R.A., and Doherty, P.C. (1997). CD8+ T cells clear influenza virus by perforin or Fas-dependent processes. J. Immunol. *159*, 5197–5200.
19. Lillie, P.J., Berthoud, T.K., Powell, T.J., Lambe, T., Mullarkey, C., Spencer, A.J., Hamill, M., Peng, Y., Blais, M.E., Duncan, C.J., et al. (2012). Preliminary assessment of the efficacy of a T-cell-based influenza vaccine, MVA-NP+M1, in humans. Clin. Infect. Dis. *55*, 19–25.
20. Houser, K., and Subbarao, K. (2015). Influenza vaccines: challenges and solutions. Cell Host Microbe *17*, 295–300.
21. Scorza, F.B., and Pardi, N. (2018). New Kids on the Block: RNA-Based Influenza Virus Vaccines. Vaccines (Basel) *6*, 20.
22. Magini, D., Giovani, C., Mangiavacchi, S., Maccari, S., Cecchi, R., Ulmer, J.B., De Gregorio, E., Geall, A.J., Brazzoli, M., and Bertholet, S. (2016). Self-Amplifying mRNA Vaccines Expressing Multiple Conserved Influenza Antigens Confer Protection against Homologous and Heterosubtypic Viral Challenge. PLoS ONE *11*, e0161193.
23. Brazzoli, M., Magini, D., Bonci, A., Buccato, S., Giovani, C., Kratzer, R., Zurli, V., Mangiavacchi, S., Casini, D., Brito, L.M., et al. (2015). Induction of Broad-Based Immunity and Protective Efficacy by Self-amplifying mRNA Vaccines Encoding Influenza Virus Hemagglutinin. J. Virol. *90*, 332–344.
24. Petsch, B., Schnee, M., Vogel, A.B., Lange, E., Hoffmann, B., Voss, D., Schlake, T., Thess, A., Kallen, K.J., Stitz, L., and Kramps, T. (2012). Protective efficacy of in vitro synthesized, specific mRNA vaccines against influenza A virus infection. Nat. Biotechnol. *30*, 1210–1216.
25. Joe, P.T., Christopoulou, I., van Hoecke, L., Schepens, B., Ysenbaert, T., Heirman, C., Thielemans, K., Saelens, X., and Aerts, J.L. (2019). Intranodal administration of mRNA encoding nucleoprotein provides cross-strain immunity against influenza in mice. J. Transl. Med. *17*, 242.
26. Hajam, I.A., Senevirathne, A., Hewawaduge, C., Kim, J., and Lee, J.H. (2020). Intranasally administered protein coated chitosan nanoparticles encapsulating

influenza H9N2 HA2 and M2e mRNA molecules elicit protective immunity against avian influenza viruses in chickens. Vet. Res. (Faisalabad) *51*, 37.

27. Pardi, N., Tuyishime, S., Muramatsu, H., Kariko, K., Mui, B.L., Tam, Y.K., Madden, T.D., Hope, M.J., and Weissman, D. (2015). Expression kinetics of nucleoside-modified mRNA delivered in lipid nanoparticles to mice by various routes. J. Control. Release *217*, 345–351.

28. Alameh, M.G., Weissman, D., and Pardi, N. (2020). Messenger RNA-Based Vaccines Against Infectious Diseases. Curr. Top. Microbiol. Immunol. Published online April 17, 2020. https://doi.org/10.1007/82_2020_202.

29. Chagla, Z. (2021). The BNT162b2 (BioNTech/Pfizer) vaccine had 95% efficacy against COVID-19 ≥7 days after the 2nd dose. Ann. Intern. Med. *174*, JC15.

30. Baden, L.R., El Sahly, H.M., Essink, B., Kotloff, K., Frey, S., Novak, R., Diemert, D., Spector, S.A., Rouphael, N., Creech, C.B., et al.; COVE Study Group (2021). Efficacy and Safety of the mRNA-1273 SARS-CoV-2 Vaccine. N. Engl. J. Med. *384*, 403–416.

31. Pardi, N., Parkhouse, K., Kirkpatrick, E., McMahon, M., Zost, S.J., Mui, B.L., Tam, Y.K., Karikó, K., Barbosa, C.J., Madden, T.D., et al. (2018). Nucleoside-modified mRNA immunization elicits influenza virus hemagglutinin stalk-specific antibodies. Nat. Commun. *9*, 3361.

32. Feldman, R.A., Fuhr, R., Smolenov, I., Mick Ribeiro, A., Panther, L., Watson, M., Senn, J.J., Smith, M., Almarsson, Ö., Pujar, H.S., et al. (2019). mRNA vaccines against H10N8 and H7N9 influenza viruses of pandemic potential are immunogenic and well tolerated in healthy adults in phase 1 randomized clinical trials. Vaccine *37*, 3326–3334.

33. John, S., Yuzhakov, O., Woods, A., Deterling, J., Hassett, K., Shaw, C.A., and Ciaramella, G. (2018). Multi-antigenic human cytomegalovirus mRNA vaccines that elicit potent humoral and cell-mediated immunity. Vaccine *36*, 1689–1699.

34. Awasthi, S., Hook, L.M., Pardi, N., Wang, F., Myles, A., Cancro, M.P., Cohen, G.H., Weissman, D., and Friedman, H.M. (2019). Nucleoside-modified mRNA encoding HSV-2 glycoproteins C, D, and E prevents clinical and subclinical genital herpes. Sci. Immunol. *4*, eaaw7083.

35. Egan, K.P., Hook, L.M., Naughton, A., Pardi, N., Awasthi, S., Cohen, G.H., Weissman, D., and Friedman, H.M. (2020). An HSV-2 nucleoside-modified mRNA genital herpes vaccine containing glycoproteins gC, gD, and gE protects mice against HSV-1 genital lesions and latent infection. PLoS Pathog. *16*, e1008795.

36. Freyn, A.W., Ramos da Silva, J., Rosado, V.C., Bliss, C.M., Pine, M., Mui, B.L., Tam, Y.K., Madden, T.D., de Souza Ferreira, L.C., Weissman, D., et al. (2020). A Multi-Targeting, Nucleoside-Modified mRNA Influenza Virus Vaccine Provides Broad Protection in Mice. Mol. Ther. *28*, 1569–1584.

37. Espeseth, A.S., Cejas, P.J., Citron, M.P., Wang, D., DiStefano, D.J., Callahan, C., Donnell, G.O., Galli, J.D., Swoyer, R., Touch, S., et al. (2020). Modified mRNA/lipid nanoparticle-based vaccines expressing respiratory syncytial virus F protein variants are immunogenic and protective in rodent models of RSV infection. NPJ Vaccines *5*, 16.

38. Krammer, F., Margine, I., Tan, G.S., Pica, N., Krause, J.C., and Palese, P. (2012). A carboxy-terminal trimerization domain stabilizes conformational epitopes on the stalk domain of soluble recombinant hemagglutinin substrates. PLoS ONE *7*, e43603.

39. Martín, J., Wharton, S.A., Lin, Y.P., Takemoto, D.K., Skehel, J.J., Wiley, D.C., and Steinhauer, D.A. (1998). Studies of the binding properties of influenza hemagglutinin receptor-site mutants. Virology *241*, 101–111.

40. Zhu, X., McBride, R., Nycholat, C.M., Yu, W., Paulson, J.C., and Wilson, I.A. (2012). Influenza virus neuraminidases with reduced enzymatic activity that avidly bind sialic Acid receptors. J. Virol. *86*, 13371–13383.

41. Margine, I., Palese, P., and Krammer, F. (2013). Expression of functional recombinant hemagglutinin and neuraminidase proteins from the novel H7N9 influenza virus using the baculovirus expression system. J. Vis. Exp. *6*, e51112.

42. De Filette, M., Martens, W., Roose, K., Deroo, T., Vervalle, F., Bentahir, M., Vandekerckhove, J., Fiers, W., and Saelens, X. (2008). An influenza A vaccine based on tetrameric ectodomain of matrix protein 2. J. Biol. Chem. *283*, 11382–11387.

43. Watanabe, T., Watanabe, S., Ito, H., Kida, H., and Kawaoka, Y. (2001). Influenza A virus can undergo multiple cycles of replication without M2 ion channel activity. J. Virol. *75*, 5656–5662.

44. Neirynck, S., Deroo, T., Saelens, X., Vanlandschoot, P., Jou, W.M., and Fiers, W. (1999). A universal influenza A vaccine based on the extracellular domain of the M2 protein. Nat. Med. *5*, 1157–1163.

45. Antrobus, R.D., Coughlan, L., Berthoud, T.K., Dicks, M.D., Hill, A.V., Lambe, T., and Gilbert, S.C. (2014). Clinical assessment of a novel recombinant simian adenovirus ChAdOx1 as a vectored vaccine expressing conserved Influenza A antigens. Mol. Ther. *22*, 668–674.

46. Nachbagauer, R., Choi, A., Hirsh, A., Margine, I., Iida, S., Barrera, A., Ferres, M., Albrecht, R.A., García-Sastre, A., Bouvier, N.M., et al. (2017). Defining the antibody cross-reactome directed against the influenza virus surface glycoproteins. Nat. Immunol. *18*, 464–473.

47. Graham, B.S., Gilman, M.S.A., and McLellan, J.S. (2019). Structure-Based Vaccine Antigen Design. Annu. Rev. Med. *70*, 91–104.

48. Schultz-Cherry, S., and Hinshaw, V.S. (1996). Influenza virus neuraminidase activates latent transforming growth factor beta. J. Virol. *70*, 8624–8629.

49. Fernández-Arjona, M.D.M., Grondona, J.M., Fernández-Llebrez, P., and López-Ávalos, M.D. (2019). Microglial activation by microbial neuraminidase through TLR2 and TLR4 receptors. J. Neuroinflammation *16*, 245.

50. Cretescu, L., Beare, A.S., and Schild, G.C. (1978). Formation of antibody to matrix protein in experimental human influenza A virus infections. Infect. Immun. *22*, 322–327.

51. Baiersdörfer, M., Boros, G., Muramatsu, H., Mahiny, A., Vlatkovic, I., Sahin, U., and Karikó, K. (2019). A Facile Method for the Removal of dsRNA Contaminant from In Vitro-Transcribed mRNA. Mol. Ther. Nucleic Acids *15*, 26–35.